Extended Abstracts of the 2009 International Conference on Solid State Devices and Materials, Sendai, 2009, pp863-864

Thermally Robust Nanocrystal Memory with Co Bio-nanodot Self-assembled Monolayer as a Charge Trap Medium on Ultrathin $LaAlO_3$ Layer

Seungjae Jung[1], Kosuke Ohara[2], Yukiharu Uraoka[2], Takashi Fuyuki[2], Ichiro Yamashita[2] and Hyunsang Hwang[1]

[1]Department of Materials Science and Engineering, Gwangju Institute of Science and Technology, 261 Cheomdan-gwagiro (Oryong-dong), Buk-gu, Gwangju 500-712, Republic of Korea, Phone: +82-62-970-2314, Fax: +82-62-970-2304, e-mail: hwanghs@gist.ac.kr

[2]Graduated School of Materials Science, Nara Institute of Science and Technology, 8916-5 Takayama, Ikoma, Nara 630-0192, Japan

1. Introduction

Nanocrystal (NC) memory has attracted as a promising replacement for floating gate memory [1,2]. However, conventional approaches to fabricate high-density and uniformly-sized NC using CVD [1], PVD [2] and ion implantation [3], still have significant difficulties. To overcome these problems, ferritin, an cage-shape protein, has been recently studied as a template for uniform-sized and well-distributed NC fabrication [4,5]. For better memory performance such as large memory window (MW) by high density of state and longer retention by deep trap energy, thermal annealing is indispensible in terms of reducing oxide NC to metallic NC, which is stored in the inner cavity of ferritin. Although higher temperature causes better reduction, significant side effect should be considered, such as retention degradation due to metal diffusion from NC to tunnel oxide [5]. This leads to the trade-off problems between large MW and memory reliability including endurance and retention characteristics.

In this study, we demonstrate thermally robust NC memory, featuring Co bio-nanodot (Co-BND) charge trap medium on ultrathin $LaAlO_3$ (LAO) layer. LAO was used as a diffusion barrier for Co diffusion during thermal annealing, as well as a buffer layer for bandgap-engineered tunnel oxide, due to its thermally stable amorphous structure and favorable energy band structure [6-7].

2. Experiments

After standard cleaning of p-Si (100) substrate, 3 nm-thermal SiO_2 was grown at 875℃. In some sample, a 1.5 nm-LAO was deposited by e-beam evaporation. UV/O_3 cleaning was performed and then the monolayer formation of 3-aminopropyl-triethoxysilane (APTES) was carried out. Using Co-BND-accommodated ferritin solution (0.5 mg/ml & pH 7) was dropped and evaporated on tunnel oxide. The outer ferritin shell was eliminated by UV/O_3 treatment. A 20 nm-PECVD SiO_2 was deposited as a blocking oxide. Then, two different annealing process were applied to both samples for reduction of Co_3O_4 to Co NC; 400℃ for 60 min (400℃-SiO_2 or 400℃-LAO), 800℃ for 10 min (800℃-SiO_2 or 800℃-LAO) in a H_2 atmosphere (H_2:N_2 = 1:10). Pt gate was formed and then conventional forming gas annealing was implemented at 400℃.

3. Results & Discussion

Schematic illustration of fabrication process is depicted in Fig. 1. Detailed process condition for synthesis and SAM formation of Co-BND was described elsewhere [8]. Fig. 2 shows zeta potentials of bare SiO_2, APTES-treated SiO_2, and APTES-treated LAO surfaces, as a function of pH. The bare SiO_2 sample shows negative zeta potential, whereas all APTES-treated samples show positive zeta potential at pH 7. Since ferritin particles have positively-charged surface at pH 7, this evidently demonstrates that ferritin adsorption is much favorable on APTES-treated surface, even on LAO. Fig. 3 and Fig. 4 represent AFM image of Co-BND SAM before outer shell elimination and SEM images of Co-BND after outer shell elimination, respectively. These results confirm successful high-density Co-BND SAM fabrication on both SiO_2 and LAO tunnel oxide. In addition, the XPS spectrum of C 1*s* indicates that chemical residue originated from organic ferritin shell is thoroughly removed by UV/O_3 treatment (Fig. 5). Fig. 6 shows the reduction dependence of Co-BND on annealing condition. Although 6 times shorter annealing is performed, 800℃-annealed Co-BND shows much higher intensity of metallic Co 2*p* peak than 450℃-annealed one. It can be inferred that the reduction process at 800℃ or higher is required to take aforementioned advantages of Co metal NC. In Fig. 7, while the sample without Co-BND shows negligible MW, other samples show large MWs more than 3.5 V. The 800℃-annealed samples tend to show larger MW. This corresponds to the result in Fig. 6. The reason why the 800℃-LAO sample shows the largest MW might be attributed to more effective reduction of Co-BND by dangling bond of adjacent highly reactive elements (La, Al) in LAO. Fig. 8 illustrates 10-year retention at 85℃, together with endurance during 10^4 cycles. The 800℃-LAO sample shows a minimum charge loss rate and the best endurance characteristic without any MW narrowing and V_{FB} up-shift. Based on these results, we suggest a simple physical model for enhanced memory properties of the 800℃-LAO sample as described in Fig. 9. In case of the 450℃-SiO_2 sample, partially-reduced Co_3O_4 NC generates relatively shallow trap. In the 800℃-SiO_2 sample, significant charge loss occurs through leakage path generated by Co diffusion. However, in the 800℃-LAO sample, LAO is considered to effectively suppress Co diffusion and thereby enhancing memory reliability. Through conductance-voltage (G-V) characterization, interface states density (D_{it}) can be calculated, as shown in Fig. 10. As expected in previous results, the 800℃-LAO sample shows the lowest D_{it}. In conclusion, the prevention of leakage path generation and the bandgap-engineering of tunnel oxide by introducing LAO might be the origins of enhanced memory reliability without sacrificing MW.

4. Summary

Thermally robust NC memory with Co-BND on ultrathin LAO was investigated. Since LAO can act as a diffusion barrier for Co diffusion, as well as a buffer layer of tunnel oxide bandgap-engineering, which is caused by its thermally stable amorphous structure and favorable energy band structure, we could achieve stable retention and endurance characteristics, while maintaining large MW.

Acknowledgments

This work was supported by the ERC Program of the MOST/KOSEF (R11-2005-048-00000-0).

References

[1] S. Tiwari et al., *Tech. Dig. - IEDM*, (**1995**) 521.
[2] Z. Liu et al., *IEEE TED*, **49** (2002) 1606.
[3] H. Hanafi et al., *IEEE TED*, **43** (1996) 1553.
[4] I. Yamashita et al., *Tech. Dig. - IEDM*, (**2006**) 447.
[5] M. Kwon et al., *Appl. Phys. Lett.*, **90** (2007) 193512.
[6] S. Jung et al., *SSDM* (**2008**) 1146.
[7] S. Lin et al., *Tech. Dig. - IEDM*, (**2008**) 843.
[8] A. Miura et al., *Nanotechnology*, **19** (2008) 255201.

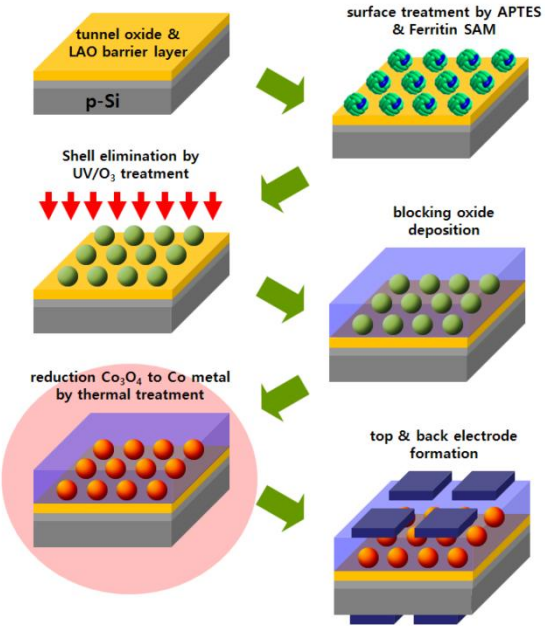

Fig. 1 Fabrication procedure of NC memory with high-density Co-BND SAM on LAO diffusion barrier, formed by using ferritin template.

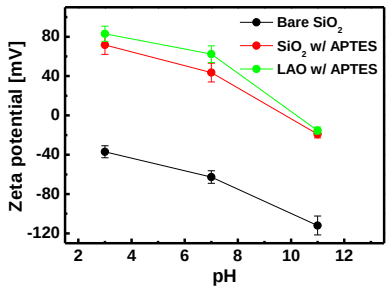

Fig. 2 Zeta potentials of bare SiO_2, APTES treated-SiO_2, and APTES-treated LAO surfaces.

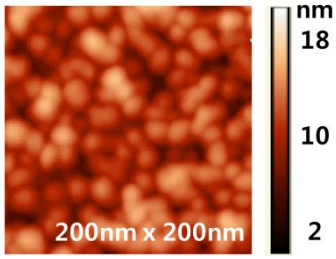

Fig. 3 AFM image of Co-BND SAM on LAO layer before ferritin shell elimination.

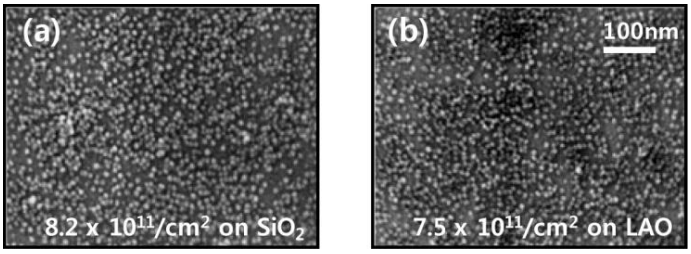

Fig. 4 SEM images of Co-BND SAM on (a) APTES-treated SiO_2 and (b) APTES-treated LAO layer after ferritin shell elimination. In SiO_2 and LAO substrate, estimated areal dot densities are 8.2×10^{11} and $7.5\times10^{11}/cm^2$, respectively.

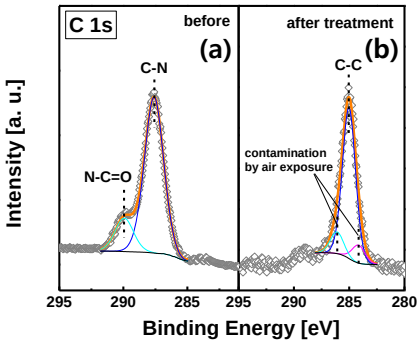

Fig. 5 C 1*s* portion of the XPS spectra of Co-BND (a) before and (b) after ferritin shell elimination. Chemical residue originated from organic ferritin shell is completely removed by UV/O_3 treatment.

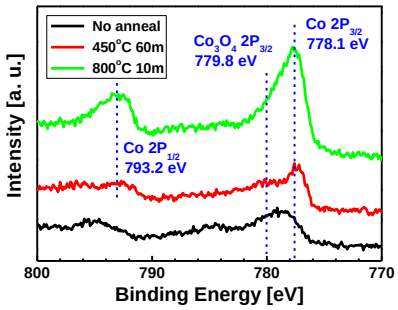

Fig. 6 Co 2*p* portions of the XPS spectra from no-, 450℃-, and 800℃-annealed Co-BND. Although shorter annealing is performed, 800℃-annealed one shows stronger reduction.

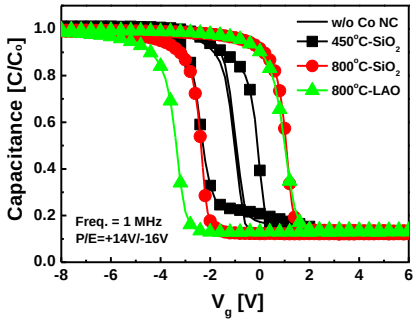

Fig. 7 MW characteristics obtained from capacitance-voltage hysteresis curves depending on annealing condition. Charge trapping efficiency of Co-BND is very sensitive to annealing condition.

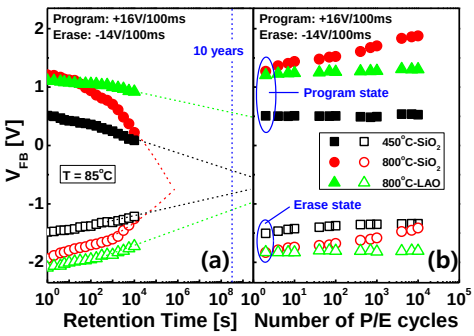

Fig. 8 (a) Retention characteristics for 10^4s at 85℃ and (b) endurance characteristics up to 10^4 cycles, depending on annealing condition.

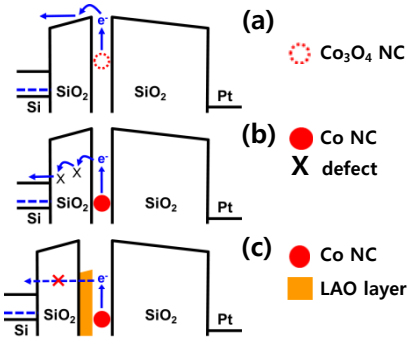

Fig. 9 The proposed physical models for the improved memory performance by introducing LAO. (a) 450℃-SiO_2, (b) 800℃-SiO_2, and (c) 800℃-LAO.

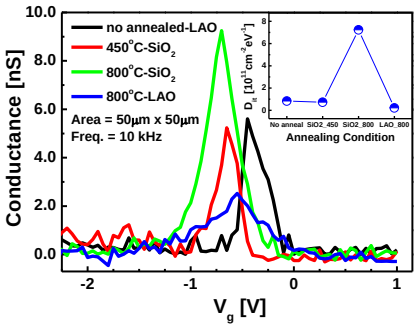

Fig. 10 G-V measurement and calculated D_{it} (inset) for each annealing conditions. D_{it} can be estimated from the position and intensity of conductance peak.